Broken chaotic clocks of brain neurons and depression

A. Bershadskii

ICAR, P.O.B. 31155, Jerusalem 91000, Israel

Irregular spiking time-series obtained *in vitro* and *in vivo* from singular brain neurons of different types of rats are analyzed by mapping to telegraph signals. Since the neural information is coded in the length of the interspike intervals and their positions on the time axis, this mapping is the most direct way to map a spike train into a signal which allows a proper application of the Fourier transform methods. This analysis shows that healthy neurons firing has periodic and chaotic deterministic clocks while for the rats representing genetic animal model of human depression these neuron clocks might be broken, that results in decoherence between the depressive neurons firing. Since depression is usually accompanied by a narrowing of consciousness this specific decoherence can be considered as a cause of the phenomenon of the consciousness narrowing as well. This suggestion is also supported by observation of the large-scale chaotic coherence of the posterior piriform and entorhinal cortices' electrical activity at transition from anesthesia to the waking state with full consciousness.

I. INTRODUCTION

All types of information, which is received by sensory system, are encoded by nerve cells into sequences of pulses of similar shape (spikes) before they are transmitted to the brain. Brain neurons use such sequences as main instrument for intercells connection. The information is reflected in the time intervals between successive firings (interspike intervals of the action potential train, see Fig. 1). There need be no loss of information in principle when converting from dynamical amplitude information to spike trains [1] and the irregular spike sequences are the foundation of neural information processing. Although understanding of the origin of interspike intervals irregularity has important implications for elucidating the temporal components of the neuronal code and for treatment of such mental disorders as depression and schizophrenia, the problem is still very far from its solution (see, for instance, Ref. [2] and references therein).

The mighty Fourier transform method, for instance, is practically non-applicable to the spike time trains. The spikes are almost identical to each other and the neural information is coded in the length of the interspike intervals and the interspike intervals positions on the time axis, therefore it is the most direct way to map the spike train into a telegraph time signal, which has values -1 from one side of a spike and values +1 from another side of the spike with a chosen time-scale resolution. An example of such mapping is given in figure 1. While the information coding is here the same as for the corresponding spike train, the Fourier transform method is quite applicable to analysis of the telegraph time-series.

On the other hand, recent dynamical models of neuron activity revealed new and complex role of regimes of a (deterministic) chaotic irregularity in the neuron spike trains (see, for instance, [3]-[6]). Therefore, we have to use all available mathematical tools in order to study the experimental data on the deterministic chaos properties
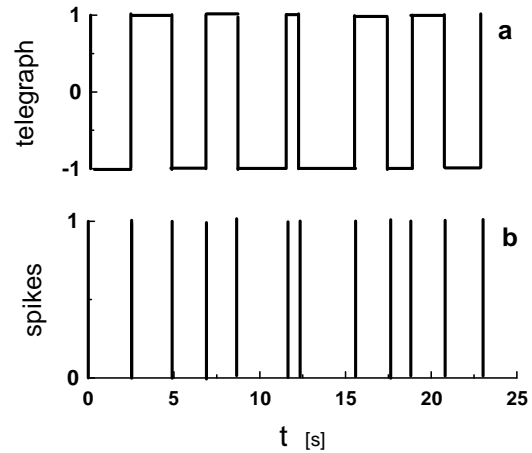

FIG. 1: Mapping of a spike train (figure 1b) into a telegraph signal (figure 1a).

(and, especially, in order to separate between deterministic chaos and stochasticity in the experimental signals).

In present paper we have analyzed three types of experimentally obtained spike trains: a) obtained *in vitro* from a spontaneous activity in CA3 hippocampal slice culture of a healthy Wistar/ST rat (the raw data and the detail description of the experiment can be found online at http://hippocampus.jp/data and in Refs. [7],[8]), b) obtained in an electrophysiological *in vivo* experiment from neurons belonging to red nucleus of a healthy (Sprague-Dawley) rat's brain (see Ref. [9] for more details of the experiment and a preliminary discussion of the data), and c) obtained in an electrophysiological *in vivo* experiment from neurons belonging to red nucleus of a genetically depressed (Flinders Sensitive Rat Line) rat's brain (see Ref. [9] for more details and a preliminary discussion of the data).

In the *in vitro* experiment a) a functional imaging technique with multicell loading of the calcium fluo-
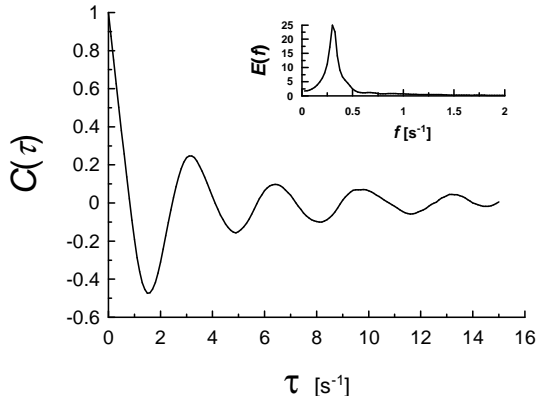
FIG. 2: Autocorrelation function for the telegraph signal corresponding to the cell-21 (800 spikes). Insert in the Fig. 2 shows corresponding spectrum.
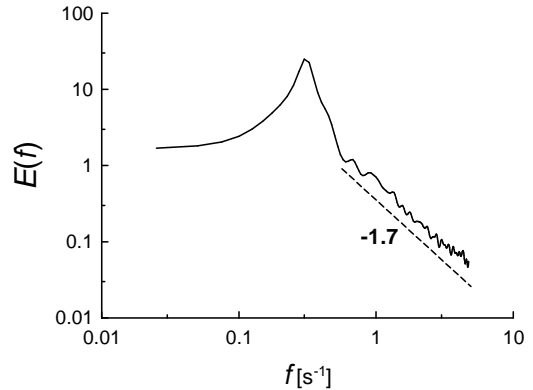

FIG. 3: Spectrum of the telegraph signal corresponding to the cell-21 in log-log scales. The dashed straight line indicates a power law: $E(f) \sim f^{-1.7}$.

rophore was used in order to obtain the spike trains of spontaneously active singular neurons in the absence of external input [7],[8]. In the *in vivo* experiments b) and c) the rats were anesthetized and the extracellular recordings were processed from the singular cells [9].

Motivation to study the hippocampus and red nucleus areas of brain in relation to the psychomotor aspects of depression is based on the recently discovered evidences of their deep involvement in this mental disorder. The hippocampus is a significant part of a brain system responsible for behavioral inhibition and attention, spatial memory, and navigation. It is also well known that spatial memory and navigation of the rats is closely related to the rhythms of their moving activity. On the other hand, the hippocampus of a human who has suffered long-term clinical depression can be as much as 20% smaller than the hippocampus of someone who has never been depressed [10]. Inputs to the Red Nucleus arise from motor areas of the brain and in particular the deep cerebellar nuclei (via superior cerebellar peduncle; crossed projection) and the motor cortex (corticorubral; ipsilateral projection). On the other hand it is known that humans with deep depression have intrinsic locomotors problems. Therefore, investigation of Red Nucleus for genetically defined rat model of depression (these rats partially resemble depressed humans because they exhibit reduced appetite and psychomotor function) can be useful for understanding the mental disorder origin.

II.   NEURON CLOCK

In the *in vitro* experiment with spontaneous activity of the hippocampal pyramidal cells different levels of activity were observed for different neurons [7],[8]. We take for our analysis the two most active neurons (http://hippocampus.jp/data - Data-006, cell-21, with
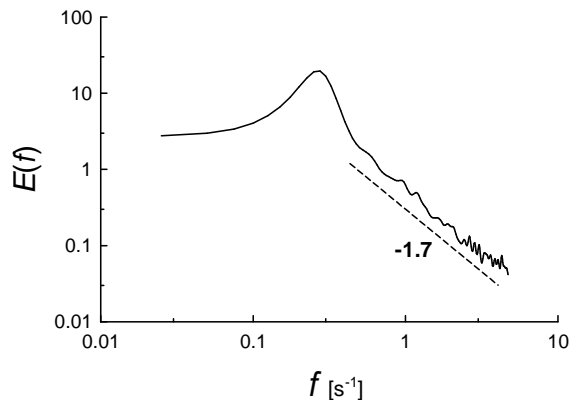

FIG. 4: As in Fig. 3 but for cell-25.

800 spikes in the time-series; and cell-25, with 692 spikes). The spike trains were mapped to telegraph signals as it is described above (see also [11]). Figure 2 shows autocorrelation function for the telegraph signal corresponding to the cell-21 (800 spikes). Insert in the Fig. 2 shows corresponding spectrum. Both the correlation function and the spectrum provide clear indication of a strong periodic component in the signal (the oscillations in the correlation function and the peak in the spectrum). The periodic component can be seen at frequency $f_0 \simeq 0.3$Hz. Figure 3 shows the spectrum in log-log scales. One can see that at high frequencies the spectrum exhibits a scaling behavior (power law: $E(f) \sim f^{-1.7}$, as indicated by the dashed straight line). The real power law can be more pronounced but under the experimental conditions individual spikes emitted at firing rates higher than 5Hz were experimentally inseparable [7],[8]. Figure 4 shows spectrum of the telegraph signal corresponding to the spike train obtained for the cell-25 (692 spikes). The spectrum is rather similar to the spectrum shown in Fig. 3 (for
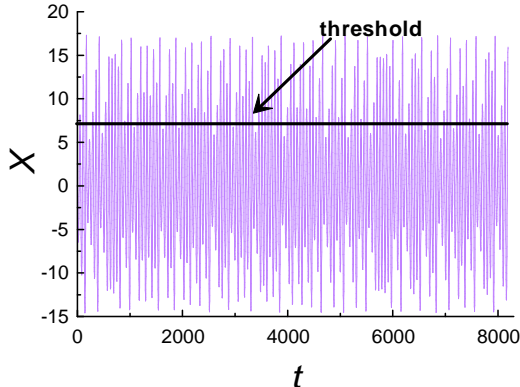
FIG. 5: X-component fluctuations of a chaotic solution of the Rössler system Eq. (1) ($a = 0.15$, $b = 0.20$, $c = 10.0$).

FIG. 6: Z-component fluctuations of a chaotic solution of the Rössler system.

cell-21). The more broad peak in Fig. 4 can be related to the poorer statistics for the cell-25 in comparison with cell-21. The spectra were calculated using the maximum entropy method (because it provides an optimal spectral resolution even for small data sets [12]).

III. THRESHOLD EFFECT

Now let us speculate about physics which could result in the spectra observed in Figs. 3 and 4. And let us recall some basic electrochemical properties of neuron. Nerve cells are surrounded by a membrane that allows some ions to pass through while it blocks the passage of other ions. When a neuron is not sending a signal it is said to be "at rest". At rest there are relatively more sodium ions onside the neuron and more potassium ions inside that neuron. The resting value of the *membrane* electrochemical potential P (the voltage difference across the neural membrane) of a neuron is about -70mV. If some event (a stimulus) causes the resting potential to move toward 0mV and the depolarization reaches about -55mV (a "normal" threshold) a neuron will fire an *action* potential. The action potential is an explosive release of charge between neuron and its surroundings that is created by a depolarizing current. If the neuron does not reach this critical threshold level, then no action potential will fire. Also, when the threshold level is reached, an action potential of a *fixed* size will always fire (for any given neuron the size of the action potential is always the same). Depending on different types of voltage-dependent ion channels, different types of action potentials are generated in different cells types and the qualitative estimates of the potentials and time periods can be varied. Recent reconstructions of a driver of the *membrane* potential using the neuron spike trains indicate the Rössler oscillator as the most probable (and simple) candidate (see, for instance, Refs. [11],[13]-[18]). Figure 5 shows as example the x-component fluctuations of a *chaotic* solution of the
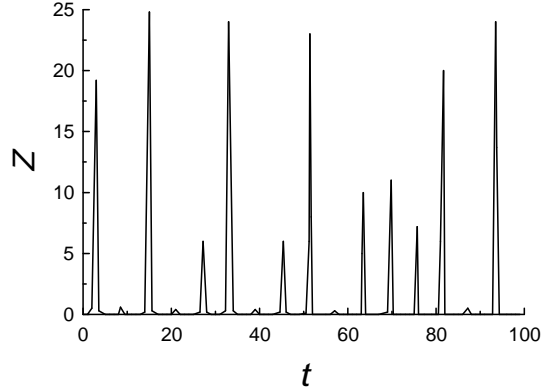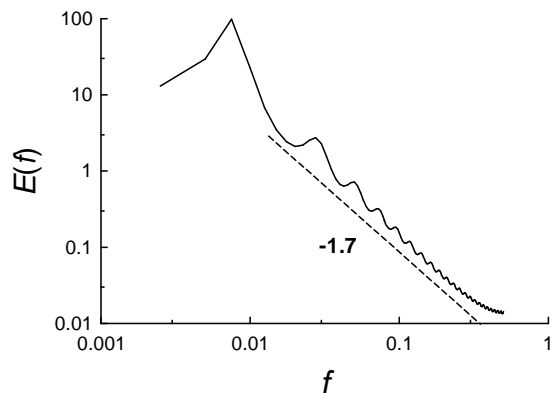

FIG. 7: Spectrum of the telegraph signal corresponding to the spike train generated by the x-component fluctuations overcoming the threshold $x = 7$. The dashed straight line indicates a power law: $E(f) \sim f^{-1.7}$.

Rössler system [19]

$$\frac{dx}{dt} = -y - z; \quad \frac{dy}{dt} = x + ay; \quad \frac{dz}{dt} = b + xz - cz \quad (1)$$

where a, b and c are parameters). At certain values of the parameters a,b and c the z-component of the Rössler system is a *spiky* time series [20],[21]: Fig. 6. It can be shown that the Rössler system and the well known Hindmarsh-Rose model [22] of neurons are subsystems of the same differential model with a spiky component [21]. Previously the 'spiky' component of such models was interpreted and studied as a simulation of a neuronal *output*. For the *spontaneous* neuron firing (without external stimulus), however, we suggest to reverse the approach and consider the spiky variable as the main component of the electrical *input* (which naturally should have a 'spiky' character, see above) to the neuron under consideration.

For each neuron the height of the spikes, which the neuron generates, is about the same. However, the heights of the spikes generated by different neurons are different. Also the signals coming from different neurons to the neuron under consideration have to go through the electrochemical passes with different properties. Therefore, the spiky z-time-series (Fig. 6) can naturally represent a multineuron signal, which can be considered as a spontaneous input for the neuron under consideration. If we use the usual interpretation of the x-component as a driver of the membrane potential $P(x)$ and the y-component as that taking into account the transport of ions across the membrane through the ion channels [22], then the position of the input (the component z) in the first equation of the system Eq. (1) has a good physical background (cf. Ref. [22]). Then, the quadratic nonlinearity in the third equation of the system Eq. (1) can be interpreted as a simple (in the Taylor expansion terms) feedback of the neuron to the main component of the neuronal input. This model with the strong nonlinear feedback can be relevant to the most active neurons of a spontaneously active brain (see below results of an *in vitro* experiment with a spontaneous brain activity). The details of the function $P(x)$ is not significant for the threshold firing process, what really matters is that the membrane potential function $P(x)$ reaches its firing value when (and only when) its argument x crosses certain threshold from below. In this simple model the driving variable x may overcome its threshold value (Fig. 5) due to the deterministic (chaotic) spontaneous stimulus. Let us consider an output spike signal resulting from overcoming a threshold value $x = 7$, for instance. Fig. 7 shows spectrum of the telegraph signal corresponding to the spike signal.

One can compare Fig. 7 with Figs. 3 and 4 to see very good reproduction of the main spectral properties.

In order to understand what is going on here we show in figure 8 spectrum of the x-component itself.

The semi-log scales are used in these figures in order to indicate exponential decay in the spectra (in the semi-log scales this decay corresponds to a straight line):

$$E(f) \sim e^{-f/f_e} \qquad (2)$$

While the peak in the spectrum corresponds to the fundamental frequency, f_0, of the Rössler chaotic attractor, the rate of the exponential decay (the slope of the straight line in Fig. 8 provides us with and additional characteristic frequency f_e. Thus Rössler chaotic attractor has two clocks: periodic with frequency f_0 and chaotic with frequency f_e. If one compares Fig. 8 and Fig. 7 one can see that the periodic clock survived the threshold crossing (with a period doubling, of course, because the only even threshold crossings in Fig. 5 result in the spike generation). The chaotic clock, however, did not survive the threshold crossing: the exponential decay in Fig. 8 has been transformed into a scaling (power law) decay in Fig. 7, which has no characteristic frequency (scale invariance). It should be noted that for a wide class of
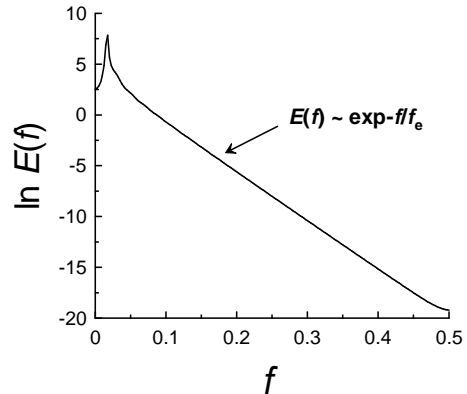

FIG. 8: Spectrum of the x-component fluctuations shown in Fig. 5. We used the semi-log axes in order to indicate exponential decay of the spectrum.
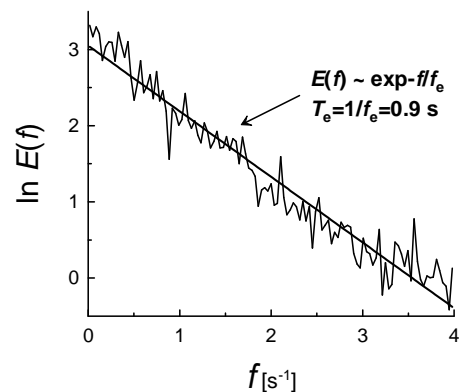

FIG. 9: Spectrum of the telegraph signal corresponding to a healthy red nucleus cell. The data is shown in the semi-log scales in order to indicate the exponential decay Eq. 2 (the straight line).
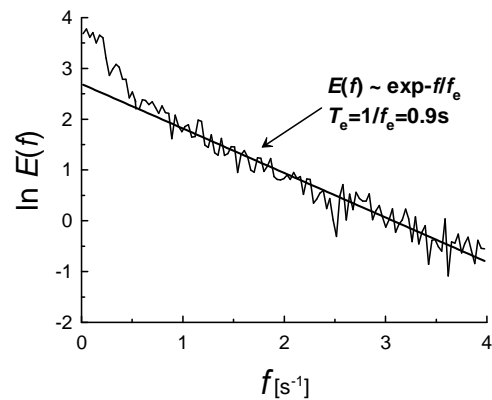

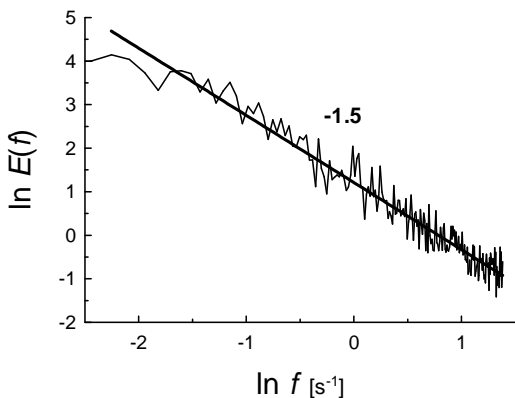FIG. 10: As in Fig. 9 but for another healthy cell.

FIG. 11: Spectrum of the telegraph signal corresponding to a genetically depressed red nucleus cell. The data is shown in the log-log scales in order to indicate the power law decay Eq. 4 (the straight line).

FIG. 12: As in Fig. 11 but for another genetically depressed red nucleus cell.

deterministic systems a broad-band spectrum with *exponential* decay is a generic feature of their *chaotic* solutions Refs. [12],[23]-[25]. It is shown in Ref. [23] that the characteristic frequency

$$f_e = \sum_i \lambda_i^+ \qquad (3)$$

where λ_i^+ are positive Lyapunov exponents of the chaotic system.

IV. CHAOS VS. STOCHASTICITY IN NEURON FIRING

Both stochastic and deterministic processes can result in the broad-band part of the spectrum, but the decay in the spectral power is different for the two cases. An exponential decay with respect to frequency refers to chaotic time series while a power-law decay indicates that the spectrum is stochastic.

Figure 9 shows a power spectrum obtained by the fast Fourier transform method applied to a telegraph signal mapped from a spike train measured in the red nucleus of a healthy rat (we can use the fast Fourier transform here due to sufficiently large number of spikes in the spike train: 2170). The spike train corresponds to a singular neuron firing. Figure 10 shows analogous spectrum obtained from another healthy red nucleus's neuron (2139 spikes). The semi-log scales are used in these figures in order to indicate exponential decay in the spectra: Eq. 2 (in the semi-log scales this decay corresponds to a straight line). The characteristic frequency $f_e \simeq 1.1$Hz in the both cases. Figure 11 shows a power spectrum obtained by the fast Fourier transform method applied to a telegraph signal mapped from a spike train (2022 spikes) measured in the red nucleus of a genetically depressive
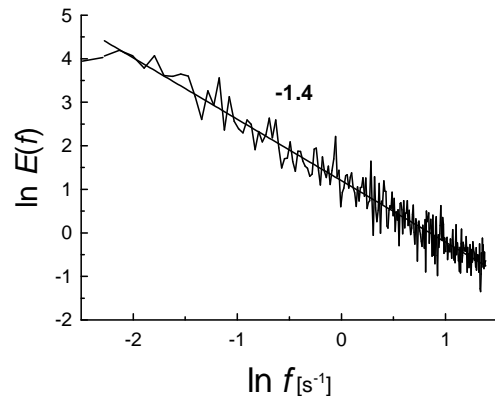
(the "Flinders" line) rat. The spike train corresponds to a singular neuron firing. Figure 12 shows analogous spectrum obtained from another genetically depressive red nucleus's neuron (2048 spikes). The log-log scales are used in these figures in order to indicate a power-law decay in the spectra (in the log-log scales this decay corresponds to a straight line):

$$E(f) \sim f^{-\alpha} \qquad (4)$$

In this (scaling) situation there is no characteristic time scale. The scaling exponent $\alpha \simeq 1.5 \pm 0.1$ and $\simeq 1.4 \pm 0.1$ for these two cases.

V. CHAOTIC NEURAL COHERENCE AND DEPRESSION

In order to work together the brain neurons have to make adjustment of their rhythms. The main problem for this adjustment is the very noisy environment of the brain neurons. If their work was based on pure periodic inner clocks this adjustment would be impossible due to the noise. The nature, however, has another option. This option is a chaotic clock. In chaotic attractors certain characteristic frequencies can be embedded by broad-band spectra, that makes them much more stable to the noise perturbations [26].

In the light of presented results one can conclude that for the considered cases the healthy neurons firing has deterministic clocks (periodic and chaotic), while the genetically depressive red nucleus's neurons exhibited a pure stochastic firing and it seems that their background deterministic clocks were broken. The existence of the background clocks can be utilized by the healthy neurons for synchronization of their activity [3],[7],[8],[27]-[29].

In order to compare coherent properties of the healthy and the depressive neuron pairs we will use cross-spectral analysis. The cross spectrum $E_{1,2}(f)$ of two processes
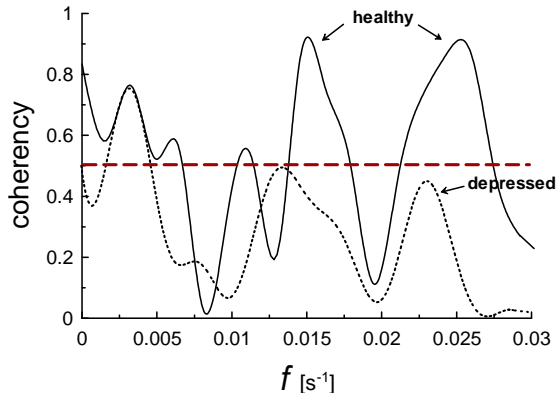
FIG. 13: Comparison of coherency in firing for the healthy (solid curve) and for the genetically depressed (doted curve) neuron pairs in a low-frequency domain (the *in vivo* experiments).
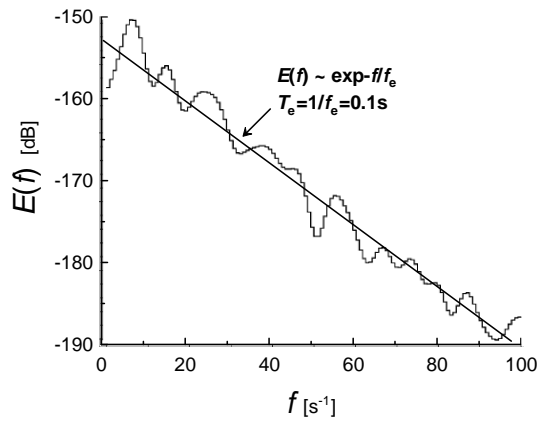

FIG. 14: Spectrum of local field potentials for the posterior piriform (adapted from Ref. [32]). The data is shown in the semi-log scales in order to indicate the exponential decay Eq. (2) (the straight line).

$x_1(t)$ and $x_2(t)$ is defined by the Fourier transformation of the cross-correlation function normalized by the product of square root of the univariate power spectra $E_1(f)$ and $E_2(f)$:

$$E_{1,2}(f) = \frac{\sum_{\tau} \langle x_1(t)x_2(t-\tau) \rangle \exp(-i2\pi f\tau)}{2\pi\sqrt{E_1(f)E_2(f)}} \quad (5)$$

the bracket $\langle ... \rangle$ denotes the expectation value. The cross spectrum can be decomposed into the phase spectrum $\phi_{1,2}(f)$ and the coherency $C_{1,2}(f)$:

$$E_{1,2}(f) = C_{1,2}(f)e^{-i\phi_{1,2}(f)} \quad (6)$$

Because of the normalization of the cross spectrum the coherency is ranging from $C_{1,2}(f) = 0$, i.e. no linear relationship between $x_1(t)$ and $x_2(t)$ at f, to $C_{1,2}(f) = 1$, i.e. perfect linear relationship.

Figure 13 shows comparison of coherency in firing for the healthy (solid curve) and for the genetically depressed (doted curve) neuron pairs in a low-frequency domain (the *in vivo* experiments). Despite of the deep anesthesia the healthy neurons exhibit bands of rather high (> 0.5) coherency in the low-frequency domain, while the depressive neurons activity is rather decoherent in this domain.

VI. LONG-RANGE CHAOTIC COHERENCE

The chaotic coherence can involve a large number of the healthy neurons and may be the entire brain. The multi-second oscillations, for instance, are known to be synchronized nearly brain-wide [30],[31]. In the case of depression, however, the chaotic neuron clocks can be broken in a significant part of the brain neurons. That can result in certain decoherence in different parts of the brain. Since depression is usually accompanied by a narrowing of consciousness (and a distorted sense of

time) this specific decoherence could be considered as a cause of the phenomenon of the consciousness narrowing as well. The coherence is important for attention, sensorimotor processing, etc.. In humans, in particular, being low in attentional flexibility magnified the effects of private self-focused attention so typical for depressive persons.

In order to support the possibility of the extended chaotic coherence we will use analysis of simultaneously recorded local field potentials from three sites along the olfactory-entorhinal axis (the anterior piriform, posterior piriform, and entorhinal cortices: aPIR, pPIR and Ent C) reported in a recent paper [32]. The measurements reported in the Ref. [32] were performed in lightly anesthetized healthy rats (the Long-Evans rats with electrode bundles implanted in their anterior and posterior cortices, and with vertical, silicon probes in their entorhinal cortices), which were emerged from the anesthesia to the waking state with full consciousness. Since the measured local field potentials time series are not spiky ones one does not need in the special data mappings in this case. The authors of the Ref. [32] discovered a new form of coherent neural activity across the three widely separated brain sites, which they named Synchronous Frequency Bursts (SFBs). The high-energy bursts of spontaneous momentary synchrony were observed across widely separated olfactory and entorhinal sites (which have also different architecture: the 6 layers of the entorhinal cortex vs. the three layers of the piriform cortices). Moreover, a significant rate of the SFBs simultaneous occurrences was also observed across the different functional processing systems: motor and olfactory ones.

The stereotypical duration of the SFBs was about 250 ms and the power spectra taken across the events were exponentially decaying. Figure 14 shows a typical
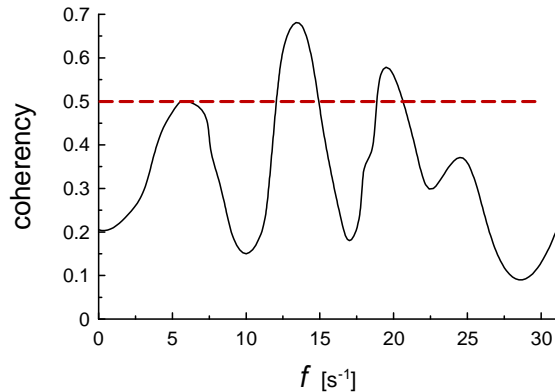
FIG. 15: Coherency calculated for the SFBs in the posterior piriform and entorhinal cortices (adapted from Ref. [32]).

spectrum for the posterior piriform area. The straight line is drawn in this figure in order to indicate the exponential decay Eq. (2) in the semi-log scales (cf. Figs. 9 and 10 for the singular neuron firing). The exponential decay indicates a chaotic nature of these bursts (see above). The decay rate $T_e = 1/f_e \simeq 0.1s$ is significantly smaller than that observed for the singular neurons (Figs. 9 and 10). Taking into account Eq. (3) one can conclude that the chaotic mixing in the phase space (determined by the Lyapunov's exponents) is much more active for the multineuron activity than for the singular neuron firing (that seems quite natural). This more active mixing shifts the spectrum into more high frequency range. Moreover, one can expect that expansion (globalization) of the chaotic coherence on the larger brain areas will shift the coherent chaotic activity even into the higher frequency ranges (cf. below).

The authors of the Ref. [32] computed coherence across SFBs in a pair of brain regions. Figure 15 shows the coherency calculated for the SFBs in the posterior piriform and entorhinal cortices (which are separated in brain space by about 8mm). One can compare this figure with the Fig. 13 (where the coherency was calculated for a pair of neighboring neurons). In this case the frequency bands of high coherency can be observed as well. The coherent frequency-range is shifted considerably in the high frequency direction for the multineuron case (see above for a reason of this shift). Actually, "the main purpose of SFBs might be to coordinate multiple frequency bands across different processing subsystems" [32]. Such *coordination* provides a sufficient level of coherence for the work of these separated subsystems with speed and efficiency impossible in the case of transmission of a specific behavioral content. This can be considered as the main advantage of the chaotic coherence. The hardware for these effective 'management' can be provided (at least partially) by recently discovered in the cortex and hippocampus interneuronal networks with long-range axonal connections [33],[34]

and for the high frequency γ-range (30-90Hz) oscillations "via neurons (and glia) inter-connected by electrical synapses called gap junctions which physically fuse and electrically couple neighboring cells."[35].

The authors of the Ref. [32] observed also that the SFBs occurrence is a function of level of consciousness. They found "that the SFBs occurred far more often under light anesthesia than deeper anesthetic states, and were especially prevalent as the animals regained consciousness". They did not observe the SFBs after the rats regained full alertness, but as they comment this can be a technical problem of inferring the specific signal from the highly complex local field potential of the awake state. Therefore, one cannot rule out the possibility that the phenomenon is still in a full swing also in the fully consciousness state (at least at certain conditions).

Finally, it should be noted that the transitional states of consciousness (emerging and decaying) have a very interesting relationship to associative human creativity (H. Poincare called these states as semi-somnolent conditions, see Ref. [36], Chapter: Mathematical discovery). The very creative and unexpected *associative* ideas that come in these states can have the above described long-range chaotic coherence as their direct physical background. Moreover, the same mechanism can also be in work at full consciousness (see previous paragraph). In this case, however, its results are considered as ones coming from the 'clear sky' and we tend to interpret them (may be wrongly) as a result of a prolonged period of unconscious work. In the full consciousness state these results are more often turn out to be adequate ones, unlike of those obtained in the transitional states [36]).

"A new result has value, if any, when, by establishing connections between elements that are known but until then dispersed and apparently unrelated to one another, order is immediately created where chaos seemed to reign" [36].

VII. ACKNOWLEDGMENTS

[1] T. Sauer, Chaos, **5**, 127 (1995).

[2] C. van Vreeswijk and H. Sompolinsky, Science, **274** (2001) 1724.

[3] E. M. Izhikevich, Dynamical Systems in Neuroscience: The Geometry of Excitability and Bursting (MIT, Cambridge, MA, 2006).

[4] G. S. Medvedev, Phys. Rev. Lett., **97**, 048102 (2006).

[5] A. Shilnikov and G. Cymbalyuk, Phys. Rev. Lett., **94**, 048101 (2005).

[6] H. Korn and P. Faure, C. R. Biologie, **326**, 787 (2003).

[7] T. Sasaki, N. Matsuki and Y. Ikegaya, J. Neuroscience, **27**, 517 (2007).

[8] N. Takahashi, T. Sasaki, W. Matsumoto, N. Matsuki, and Y. Ikegaya, PNAS, **107**, 10244 (2010).

[9] A. Bershadskii, E. Dremencov, D. Fukayama and G. Yadid, Phys. Lett. A, **289**, 337 (2001).

[10] J.D. Bremner, M. Narayan, E.R Anderson et al., Am. J. Psychiatry, **157**, 115 (2000).

[11] A. Bershadskii and Y. Ikegaya, arXiv:1010.4722 (available at http://arxiv.org/abs/1010.4722) (2010).

[12] N. Ohtomo, K. Tokiwano, Y. Tanaka et. al., J. Phys. Soc. Jpn. **64** 1104 (1995).

[13] R. Castro and T. Sauer, Phys. Rev. E, **59**, 2911 (1999).

[14] N. Masuda, and K. Aihara, Phys. Rev. Lett., **88** 248101 (2002).

[15] K. Aihara and I. Tokuda, Phys. Rev. E, **66**, 026212 (2002)

[16] T. Gedeon , M. Holzer, and M. Pernarowski, Physica D, **178**, 267 (2007)

[17] N. Crook, W.J. Goh, and M. Hawarat, BioSystems, **87**, 267 (2007).

[18] T. Pereira , M.S. Baptista, and J. Kurths, Phys. Lett. A, **362** 159 (2007).

[19] O.E. Rössler, Phys. Lett. A, **57** 397 (1976).

[20] C. Lainscsek, C.Letellier and I. Gorodnitsky, Phys. Lett. A, **314** 409 (2003).

[21] C. Lainscsek, I. Gorodnitsky and C. Letellier, Reconstructing dynamics from amplitude measures of spiky time-series, 8th Joint Symposium on Neural Computation, (2001) (available at http://www.its.caltech.edu/∼jsnc/2001/Proceedings/).

[22] J.L. Hindmarsh and R.M. Rose, Proc. R. Soc. Lond. B, **221**, 87 (1984).

[23] D.E. Sigeti, Phys. Rev. E, **52**, 2443; Physica D, **82**, 136 (1995).

[24] J. D. Farmer, Physica D, **4**, 366 (1982).

[25] U. Frisch and R. Morf, Phys. Rev., **23**, 2673 (1981).

[26] M. I. Rabinovich, and H. D. I. Abarbanel, Neuroscience, **87**, 5 (1998).

[27] D.I. Abarbanel, R. Huerta, M. I. Rabinovich, et al.,, Neural Comput., **8**, 1567 (1996).

[28] F. Mormann, K. Lehnertz, P. David, et al., Physica D, **144**, 358 (2000).

[29] E. Rossoni, Y. Chen, M. Ding, et al., Phys. Rev. E, **71**, 061904 (2005).

[30] D. Contreras, and M. Steriade, J. Neurosci., **15**, 604 (1995).

[31] M. Steriade, C Neuroscience **101** 243 (2000).

[32] R. Hermer-Vazquez, L. Hermer-Vazquez, and S. Srinivasan, Brain Res. Bull., **79**, 6(2009).

[33] T. Klausberger, P. Somogyi, Science, **321** 53 (2008).

[34] S. Jinno, T. Klausberger, L.F. Marton, et al., J. Neurosci. **27** 8790 (2007).

[35] S. Hameroff, J. Biol. Phys., **36**, 7193 (2010).

[36] H. Poincare, Science and Method (Courier Dover Publications, NY, 2003).